Interevent Correlations from Avalanches Hiding Below the Detection Threshold

Sanja Janićević,[1] Lasse Laurson,[1,2,*] Knut Jørgen Måløy,[3] Stéphane Santucci,[3,4] and Mikko J. Alava[1]
[1]COMP Centre of Excellence, Department of Applied Physics, Aalto University, P.O. Box 11100, 00076 Aalto, Espoo, Finland
[2]Helsinki Institute of Physics, Department of Applied Physics, Aalto University, P.O. Box 11100, 00076 Aalto, Espoo, Finland
[3]Department of Physics, University of Oslo, PB 1048 Blindern, Oslo NO-0316, Norway
[4]Laboratoire de Physique, CNRS UMR 5672, Ecole Normale Supérieure de Lyon, 46 Allée d'Italie, 69364 Lyon Cedex 07, France
(Received 5 July 2016; published 1 December 2016)

Numerous systems ranging from deformation of materials to earthquakes exhibit bursty dynamics, which consist of a sequence of events with a broad event size distribution. Very often these events are observed to be temporally correlated or clustered, evidenced by power-law-distributed waiting times separating two consecutive activity bursts. We show how such interevent correlations arise simply because of a finite detection threshold, created by the limited sensitivity of the measurement apparatus, or used to subtract background activity or noise from the activity signal. Data from crack-propagation experiments and numerical simulations of a nonequilibrium crack-line model demonstrate how thresholding leads to correlated bursts of activity by separating the avalanche events into subavalanches. The resulting temporal subavalanche correlations are well described by our general scaling description of thresholding-induced correlations in crackling noise.

DOI: 10.1103/PhysRevLett.117.230601

A large class of physical, biological, and other systems respond to slowly changing external conditions by exhibiting scale-free avalanche dynamics, or "crackling noise" [1], measurable as a bursty activity signal $V(t)$. Depending on the system, $V(t)$ may originate from a number of processes: the velocity of a propagating crack [2–5] or the plastic deformation rate [6–10] in a stressed solid, the fluid invasion rate into porous media [11,12], the rate of change of magnetization in a dirty ferromagnet in a slowly changing external magnetic field [13,14], or time-dependent activity in neuronal networks [15,16]. In many cases, the critical-like scaling implied by the power-law burst-size distributions has found an interpretation in terms of a nonequilibrium phase transition [17], separating quiescent and active phases of the system [18], and making it possible to apply concepts and tools such as universality and renormalization group theory [19].

Another key feature of typical crackling noise signals is that the bursts often exhibit temporal correlations, visible as power-law-distributed waiting times (quiet times, or periods of low activity) separating two consecutive events [20–26]; in contrast to these observations, uncorrelated triggering of avalanches would be described by a Poisson process, with exponentially distributed waiting times. The perhaps best-known example of such temporal correlations is the spatiotemporal clustering of earthquakes [20], often described by phenomenological laws like the Omori law [27,28]. Similar time clustering of events or power-law-distributed waiting times are also observed in acoustic [21,22] and light [23] emission from fracture, compression of wood samples [24], and porous materials [25], as well as for neuronal avalanches [26].

From a theoretical perspective, the typical quasistatically driven model systems (of propagating cracks, invasion fronts, domain walls, etc.), where the bursty activity stems from an underlying dynamical phase transition, fail to reproduce the empirically observed strong temporal interevent correlations, thus raising the question of their origin. If one incorporates additional slow processes [29] (e.g., viscoelasticity [30]) in these models, temporal avalanche clustering may be recovered. However, such attempts merely call for more general explanations of the empirical observations of interevent temporal correlations in a variety of crackling noise systems.

By using experimental data from planar crack-propagation experiments and numerical simulations of a crack-line model, we show how temporal avalanche correlations in crackling noise simply result from the thresholding process used to define the bursts or avalanches [31,32]. This thresholding is often necessary: it is applied either indirectly (due to a finite detection threshold or sensitivity of the experimental apparatus) or actively [when finite activity background or noise level needs to be subtracted from $V(t)$ to look for avalanches]. The full avalanche events—which are correlated sequences of activity by definition—are partly "hiding" below the finite detection threshold, and thus broken into subavalanches in the thresholding process. This leads to correlations between the observed events, even if the underlying "true" avalanche triggers can be well described by a Poisson process. We present a general scaling description of the thresholding-induced (sub)avalanche correlations, and find that our experimental and numerical results are in excellent agreement with the resulting predictions.

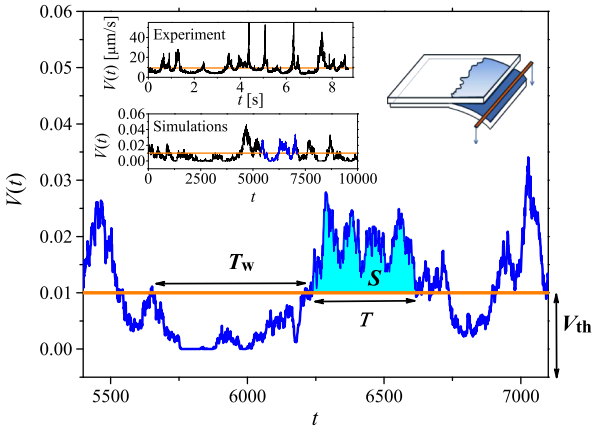

FIG. 1. Insets on the left show examples of the experimental (top) and numerical (bottom) crack-front velocity time series $V(t)$. The blue part of the latter is shown magnified in the main figure, with definitions of the avalanche size S, duration T, and waiting time T_W, resulting from applying a finite threshold level V_{th} (orange line). The geometry of the experiment is portrayed in the top right inset.

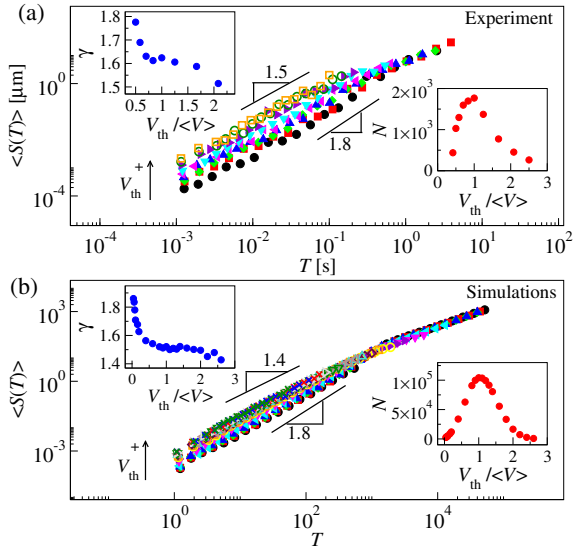

FIG. 2. Scaling of $\langle S(T)\rangle$ with T for a wide range of threshold levels V_{th}, with arrows indicating the direction of rising V_{th}. The experimental data for $\langle V\rangle = 10.2\ \mu$m/s and for V_{th} varied in the range 5.1–25.5 μm/s are shown in panel (a), with the corresponding numerical results for $\langle V\rangle = 0.025$ and V_{th} in the range 0.001–0.065 in panel (b). The top-left insets show the evolution of the effective value of γ with V_{th}, resulting from a fit to the scaling range of the $\langle S(T)\rangle$ data. The bottom-right insets display the V_{th} dependence of the number of (sub)avalanches, exhibiting a maximum at $V_{\mathrm{th}} \approx \langle V\rangle$.

When defining bursts or avalanches from a bursty signal $V(t)$ by thresholding, a finite threshold level V_{th} is imposed, and excursions of $V(t)$ above V_{th} are identified as events of interest, see Fig. 1. Their sizes $S = \int_0^T dt[V(t) - V_{\mathrm{th}}]$ and durations T are power-law distributed with a cutoff, that is, $P(S) = S^{-\tau_S} f(S/S_0)$ and $P(T) = T^{-\tau_T} g(T/T_0)$, with $f(x)$ and $g(x)$ scaling functions, and S_0 and T_0 the cutoff avalanche size and duration, respectively. The average avalanche size scales with the duration as $\langle S(T)\rangle \propto T^{\gamma}$, with the critical exponents expected to satisfy the scaling relation $\gamma = (\tau_T - 1)/(\tau_S - 1)$. The average burst amplitude would then scale as $T^{\gamma-1}$ [4].

When applying a finite V_{th}, $V(t)$ will also have excursions below V_{th} (see again Fig. 1), with corresponding time intervals T_W referred to as the waiting times. In the simplest possible scaling picture, the excursions above and below V_{th} would have the same statistical properties up to a cutoff scale. Such a symmetry applies in the scaling regime of memory-less Markovian processes, such as simple random walks [31], but the same may also be true for critical avalanches due to their self-affine properties. The visually asymmetric appearance of the $V(t)$ signals with respect to V_{th} (Fig. 1) can be understood by noticing that the cutoff mechanisms acting on excursions above and below V_{th} are different: the stiffness parameter K (or, e.g., the demagnetizing factor in the case of bursty dynamics of domain walls) results in a "soft" cutoff mechanism that limits the growth of $V(t)$ above V_{th}, giving rise to a cutoff avalanche duration $T_0 \propto K^{-1/\sigma_K}$. The constraint $V(t) \geq 0$ acts as a "hard" cutoff for excursions of $V(t)$ below V_{th}, leading to a cutoff waiting time $T_{W,0}$. In the scaling regime, i.e., for $T \ll T_0$ and $T_W \ll T_{W,0}$, we expect the statistical properties of the waiting times T_W to be similar to avalanche durations T; that is, $P(T_W)$ should be a power law with a cutoff

$$P(T_W) = T_W^{-\tau_{T_W}} g'\left(\frac{T_W}{T_{W,0}}\right), \tag{1}$$

with $g'(x)$ another scaling function. Because of the conjectured symmetry between the excursions of $V(t)$ above and below V_{th}, $\tau_{T_W} = \tau_T$. The boundary condition at $V(t) = 0$, together with the symmetry of the excursions above and below V_{th}, leads to a cutoff waiting time $T_{W,0}$ obeying $V_{\mathrm{th}} \propto T_{W,0}^{\gamma-1}$. Thus $T_{W,0} \propto V_{\mathrm{th}}^{\delta}$, where $\delta = 1/(\gamma - 1)$. Because usually $\gamma > 1$, $T_{W,0}$ thus increases with rising V_{th}. These predictions originate from the hypothesis that empirical observations of power-law waiting-time distributions are due to avalanches partly hiding below the detection threshold. Next, we proceed to test these predictions for experimental and numerical data on bursty crack propagation in disordered solids.

In the experiments, a crack is forced to propagate along a heterogeneous weak plane of a transparent poly(methyl methacrylate) block with an imposed constant velocity $\langle V\rangle$ in quasimode I geometry [2–4]. A high-resolution fast camera mounted on a microscope directly observes the interfacial crack growth (Fig. 1, right inset). The measured

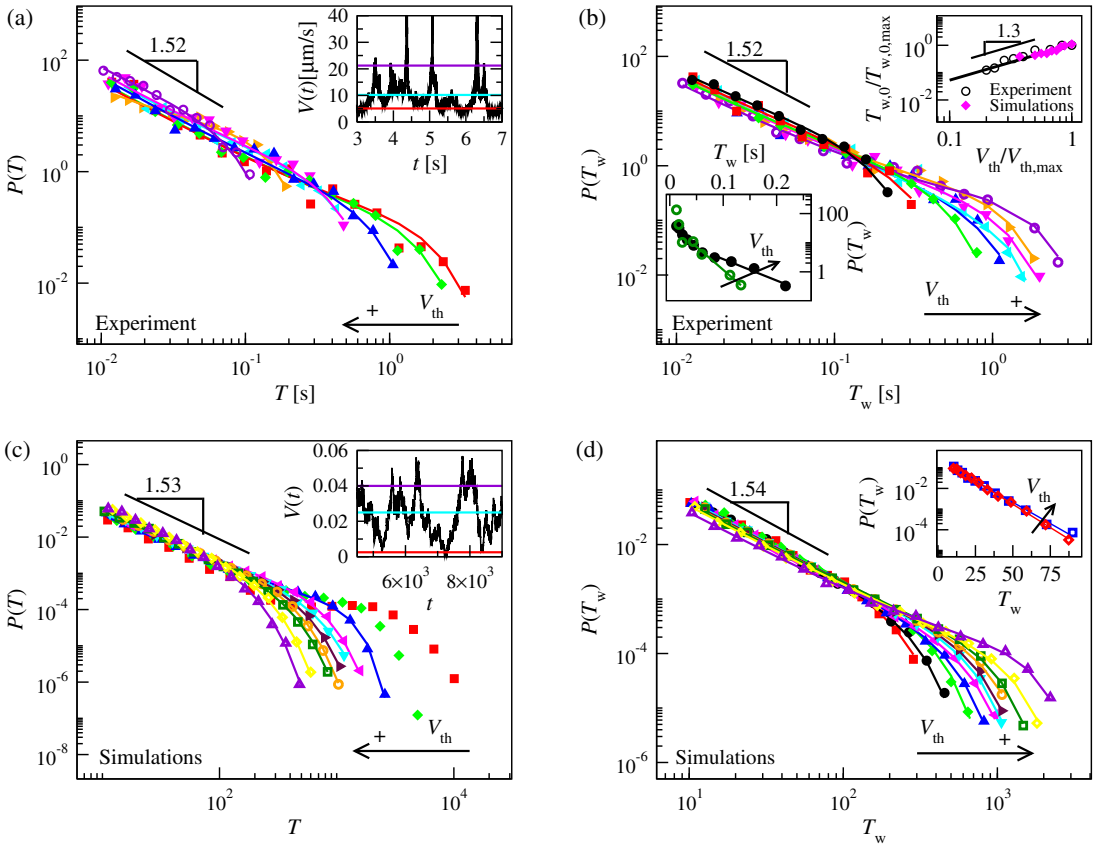

FIG. 3. Panels (a) and (b) show experimental $P(T)$ and $P(T_W)$ distributions, respectively, for $\langle V\rangle = 10.2$ μm/s and a wide range of V_{th}s, with arrows indicating the direction of rising V_{th}; the corresponding data from simulations are shown in panels (c) and (d), with $\langle V\rangle = 0.025$. The horizontal lines in the insets of (a) and (c) illustrate the maximum and minimum V_{th} used, as well as $\langle V\rangle$, showing a typical part of the $V(t)$ signal for reference. $P(T_W)$ evolves from an exponential [bottom-left inset of (b) and the inset of (d) show examples for even smaller V_{th}s than in the main panel(s) on a semilog scale] to a power law with a cutoff as V_{th} is increased; τ_{T_W} equals $\tau_T = 1.53 \pm 0.05$ within error bars. The cutoff $T_{W,0}$ of the waiting-time distributions grows with V_{th} as $T_{W,0} \propto V_{th}^{\delta}$, with $\delta \approx 1.3$ [top-right inset of (b), showing data from both simulations and experiment]. Solid lines in the main panels correspond to fits of Eq. (S1) discussed in the Supplemental Material [35].

crackling noise (Fig. 1, top-left inset) corresponds to the time evolution $V(t)$ of the spatially averaged crack-front velocity; it has been shown to display intermittent avalanche dynamics with complex spatiotemporal interevent correlations [2,4,33,34]. For more details, see the Supplemental Material [35].

The large-scale dynamics of our planar crack experiment can be described by a model of a long-range elastic, one-dimensional (1D) string propagating in a 2D random medium [4,5,41,42]. Here, we perform an extensive set of simulations of its discretized version, known to capture the avalanche statistics of the corresponding continuous model [4,5,41], and represented by a set of integer heights $h_i(t)$, $i = 1, \ldots, L$, with L the system size. The lateral coordinates x_i of the interface are given by $x_i = i$. The total force acting on the interface element i is

$$F_i = \Gamma_0 \sum_{j \neq i} \frac{h_j - h_i}{|x_j - x_i|^2} + \eta(x_i, h_i) + F_{\text{ext}}, \qquad (2)$$

where the first term on the right-hand side represents the long-range elastic interactions, η is uncorrelated quenched disorder modeling toughness fluctuations of the disordered weak plane, and F_{ext} is the external driving force. In addition to planar crack-front propagation [4,5,41], the model also describes contact lines of liquids spreading on solid surfaces [43,44] and low-angle grain boundaries in plastically deforming crystals [45]. The crackling noise signal is given by $V(t) = 1/L \sum_i v_i(t)$, where $v_i = \theta(F_i)$, with θ the Heaviside step function. The interface is driven with a constant velocity $\langle V\rangle$, by imposing $F_{\text{ext}} = K(\langle V\rangle t - \langle h\rangle)$, where K describes the stiffness of the specimen-machine system and controls the cutoffs S_0 and T_0, and $\langle h\rangle$ is the average interface height. For additional details, see the Supplemental Material [35].

First, we consider the scaling of the average avalanche size $\langle S(T)\rangle$ with the avalanche duration T for different threshold levels V_{th}. Figure 2(a), in which experimental data with $\langle V\rangle = 10.2$ μm/s are considered, shows that the effective γ value depends on V_{th} [top-left inset of Fig. 2(a),

and Supplemental Material, Fig. S1 [35]]; the theoretically expected value, $\gamma \approx 1.8$ [4], is recovered only in the limit $V_{\rm th} \ll \langle V \rangle$, while larger $V_{\rm th}$ values lead to smaller effective values of γ. In particular, using a $V_{\rm th}$ maximizing the number of events [this happens for $V_{\rm th} \approx \langle V \rangle$, a typical choice in experiments, see the bottom right inset of Fig. 2(a)] would lead to a γ value different from the one obtained in the low-threshold limit. Figure 2(b) shows that the threshold dependence of the $\langle s(T) \rangle$ scaling observed for the experimental data is captured by the model.

Next, we present how power-law-distributed waiting times in crackling noise emerge from thresholding. To this end, Figs. 3(a) and 3(b) show examples of the experimental $P(T)$ and $P(T_W)$ distributions, respectively, for a wide range of threshold levels $V_{\rm th}$. The (sub)avalanche duration distributions $P(T)$ display a power law terminated at a cutoff T_0, with the latter decreasing with increasing $V_{\rm th}$. Also the $P(T_W)$ distributions display a power law with a cutoff, exhibiting the opposite trend to $P(T)$ distributions in that the cutoff scale $T_{W,0}$ increases with $V_{\rm th}$ as $T_{W,0} \propto V_{\rm th}^{\delta}$, with $\delta = 1.30 \pm 0.10$ [top-right inset of Fig. 3(b)]; this corresponds to $\gamma \approx 1.77 \pm 0.06$, that is, close to the low-threshold result quoted above from the $\langle S(T) \rangle$ scaling. Notably, for very small $V_{\rm th}$, $P(T_W)$ ceases to have a power-law part and is instead close to a pure exponential [bottom-left inset of Fig. 3(b)], indicating that the "true" avalanche triggers would be well described by an uncorrelated Poisson process [30]. Upon increasing $V_{\rm th}$, avalanches more frequently break into subavalanches, and a power-law part emerges, characterized by an exponent $\tau_{T_W} \approx \tau_T = 1.52 \pm 0.05$, signaling the onset of apparent correlations due to thresholding. These results can be reproduced in experiments with other $\langle V \rangle$ values (Supplemental Material, Figs. S2 and S3 [35]).

Figures 3(c) and 3(d) show examples of the corresponding numerical $P(T)$ and $P(T_W)$ distributions. We observe an excellent agreement between simulation and experimental results, with $P(T_W)$ evolving from an exponential to a power law with increasing $V_{\rm th}$. The exponent τ_{T_W} equals $\tau_T = 1.52 \pm 0.03$ within error bars, and $T_{W,0}$ increases with $V_{\rm th}$ as $T_{W,0} \propto V_{\rm th}^{1.3}$ [(filled symbols in the top-right inset of Fig. 3(b)]. The areas S and $S' = \int_0^{T_W} dt[V_{\rm th} - V(t)]$ of the excursions of $V(t)$ above and below $V_{\rm th}$, respectively, scale with the same exponent $\tau_S = \tau_{S'} \approx 1.28$ (Supplemental Material, Fig. S4 [35]). We also note that a mean-field version of Eq. (2) agrees with our scaling picture (Supplemental Material, Figs. S5 and S6 [35]).

This excellent agreement between experiment and model allows us to apply the latter to probe the quasistatic limit $\langle V \rangle \to 0$, which is not easily reachable experimentally. Figure 4 shows the simulated $P(T_W)$ distributions for a wide range of $\langle V \rangle$ values, setting $V_{\rm th} = \langle V \rangle$. When $V_{\rm th} = \langle V \rangle \to 0$, $P(T_W)$ becomes an exponential with a long characteristic waiting time, and evolves towards a power law with increasing $V_{\rm th} = \langle V \rangle$. This provides an additional way of looking at how the thresholding process results in a power law $P(T_W)$, even if the underlying "true" avalanches are triggered by a Poisson process.

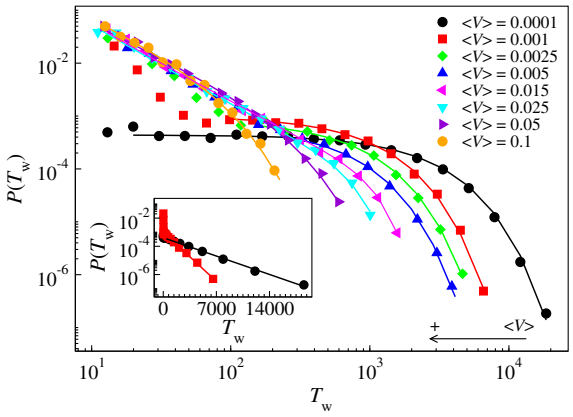

FIG. 4. The numerically simulated $P(T_W)$ distributions for a wide range of $\langle V \rangle$, with $V_{\rm th} = \langle V \rangle$. Upon decreasing $\langle V \rangle$ (and, thus, $V_{\rm th}$), $P(T_W)$ evolves from a power law with a cutoff towards a purely exponential distribution (see the inset for the two distributions with the smallest $\langle V \rangle$ with a semilog axis scale), indicating the absence of correlation in the limit $\langle V \rangle$, $V_{\rm th} \to 0$. Solid lines in the main panel correspond to fits of Eq. (S1) discussed in the Supplemental Material [35].

Our results show that when bursty events are extracted from a crackling noise signal by thresholding, they tend to exhibit apparent temporal correlations visible as power-law-distributed waiting times. While noise-filtering techniques [46] may be applied to reduce the need of thresholding of $V(t)$ signals suffering from experimental noise, finite sensitivity of any real measurement should lead to a similar outcome. This viewpoint agrees with the fact that a large fraction of empirical crackling noise signals exhibit power-law waiting-time distributions. Indeed, we expect our arguments to be generally applicable for any system exhibiting crackling noise, ranging from Barkhausen noise in ferromagnets to earthquakes. The importance of seismic activity below the detection threshold for earthquake statistics has been discussed by suggesting that small, undetectable shocks may trigger detectable events [47]. Our interpretation would, however, be more far reaching, suggesting that temporally correlated (or clustered) events may be parts of the same avalanche. Our Letter shows how to test this *a posteriori* by varying the threshold applied to define the crackling-noise events. When performing such tests, one should bear in mind that strong-enough additive white noise in the $V(t)$ signal (e.g., due to noisy experimental apparatus) is expected to result in scaling properties of the waiting times different from the ones reported here [31]. Our crack-propagation experiments have the advantage of very low levels of experimental noise, and, thus, our experimental results adhere to the noise-free scaling picture of thresholding-induced waiting times.

Moreover, other processes may be operating in some systems [30] in parallel with the thresholding-induced

event clustering, and are likely to lead to different types of correlations not fully accounted for by our scaling description; an interesting possibility would be to modify our experiment—by changing the material and/or the experimental conditions—to add viscoelastic response to the system. Thus, our work calls for detailed analysis of experimental data in diverse crackling-noise systems to decipher the origin and nature of interevent correlations or avalanche clustering in each case.

This research has been supported by the Academy of Finland through an Academy Research Fellowship (L. L., Project No. 268302) and through the Centres of Excellence Program (Project No. 251748). K. J. M. acknowledges the support of the Norwegian Research Council through the Frinat Grant No. 205486. L. L. wishes to thank S. S. and CNRS for the hospitality during the invited researcher visit at ENS Lyon. We acknowledge the computational resources provided by the Aalto University School of Science "Science-IT" project.

*lasse.laurson@aalto.fi

[1] J. P. Sethna, K. Dahmen, and C. R. Myers, Crackling noise, Nature (London) **410**, 242 (2001).
[2] J. Schmittbuhl and K. J. Måløy, Direct Observation of a Self-Affine Crack Propagation, Phys. Rev. Lett. **78**, 3888 (1997).
[3] K. J. Måløy, S. Santucci, J. Schmittbuhl, and R. Toussaint, Local Waiting Time Fluctuations along a Randomly Pinned Crack Front, Phys. Rev. Lett. **96**, 045501 (2006).
[4] L. Laurson, X. Illa, S. Santucci, K. T. Tallakstad, K. J. Måløy, and M. J. Alava, Evolution of the average avalanche shape with the universality class, Nat. Commun. **4**, 2927 (2013).
[5] L. Laurson, S. Santucci, and S. Zapperi, Avalanches and clusters in planar crack front propagation, Phys. Rev. E **81**, 046116 (2010).
[6] M. J. Alava, L. Laurson, and S. Zapperi, Crackling noise in plasticity, Eur. Phys. J. Spec. Top. **223**, 2353 (2014).
[7] M. Zaiser, Scale invariance in plastic flow of crystalline solids, Adv. Phys. **55**, 185 (2006).
[8] M. C. Miguel, A. Vespignani, S. Zapperi, J. Weiss, and J. R. Grasso, Intermittent dislocation flow in viscoplastic deformation, Nature (London) **410**, 667 (2001).
[9] D. M. Dimiduk, C. Woodward, R. LeSar, and M. D. Uchic, Scale-free intermittent flow in crystal plasticity, Science **312**, 1188 (2006).
[10] F. Csikor, C. Motz, D. Weygand, M. Zaiser, and S. Zapperi, Dislocation avalanches, strain bursts, and the problem of plastic forming at the micrometer scale, Science **318**, 251 (2007).
[11] M. Rost, L. Laurson, M. Dubé, and M. J. Alava, Fluctuations in Fluid Invasion into Disordered Media, Phys. Rev. Lett. **98**, 054502 (2007).
[12] S. Santucci, R. Planet, K. J. Måløy, and J. Ortin, Local avalanche dynamics of imbibition fronts: Towards critical pinning, Europhys. Lett. **94**, 46005 (2011).
[13] G. Durin and S. Zapperi, *The Science of Hysteresis*, edited by G. Bertotti and I. Mayergoyz (Academic Press, Amsterdam, 2006), pp. 181–267.
[14] G. Durin and S. Zapperi, Scaling Exponents for Barkhausen Avalanches in Polycrystalline and Amorphous Ferromagnets, Phys. Rev. Lett. **84**, 4705 (2000).
[15] J. M. Beggs and D. Plenz, Neuronal avalanches in neocortical circuits, J. Neurosci. **23**, 11167 (2003).
[16] T. Bellay, A. Klaus, S. Seshadri, and D. Plenz, Irregular spiking of pyramidal neurons organizes as scale-invariant neuronal avalanches in the awake state, eLife **4**, e07224 (2015).
[17] S. Lübeck, Universal scaling behavior of nonequilibrium phase transitions, Int. J. Mod. Phys. B **18**, 3977 (2004).
[18] D. S. Fisher, Collective transport in random media: from superconductors to earthquakes, Phys. Rep. **301**, 113 (1998).
[19] P. Le Doussal and K. J. Wiese, Size distributions of shocks and static avalanches from the functional renormalization group, Phys. Rev. E **79**, 051106 (2009).
[20] Y. Ben-Zion, Collective behavior of earthquakes and faults: Continuum-discrete transitions, progressive evolutionary changes, and different dynamic regimes, Rev. Geophys. **46**, RG4006 (2006).
[21] L. I. Salminen, A. I. Tolvanen, and M. J. Alava, Acoustic Emission from Paper Fracture, Phys. Rev. Lett. **89**, 185503 (2002).
[22] M. Stojanova, S. Santucci, L. Vanel, and O. Ramos, High Frequency Monitoring Reveals Aftershocks in Subcritical Crack Growth, Phys. Rev. Lett. **112**, 115502 (2014).
[23] A. Tantot, S. Santucci, O. Ramos, S. Deschanel, M.-A. Verdier, E. Mony, Y. Wei, S. Ciliberto, L. Vanel, and P. C. F. Di Stefano, Sound and Light from Fractures in Scintillators, Phys. Rev. Lett. **111**, 154301 (2013).
[24] T. Mäkinen, A. Miksic, M. Ovaska, and M. J. Alava, Avalanches in Wood Compression, Phys. Rev. Lett. **115**, 055501 (2015).
[25] J. Baró, A. Corral, X. Illa, A. Planes, E. K. H. Salje, W. Schranz, D. E. Soto-Parra, and E. Vives, Statistical Similarity Between the Compression of a Porous Material and Earthquakes, Phys. Rev. Lett. **110**, 088702 (2013).
[26] D. Plenz and D. R. Chialvo, Scaling properties of neuronal avalanches are consistent with critical dynamics, arXiv: 0912.5369.
[27] F. Omori, On the aftershocks of earthquakes, J. Coll. Sci. Imp. Univ. Tokyo **7**, 111 (1894).
[28] L. de Arcangelis, C. Godano, J. R. Grasso, and E. Lippiello, Statistical physics approach to earthquake occurrence and forecasting, Phys. Rep. **628**, 1 (2016).
[29] S. Papanikolaou, D. M. Dimiduk, W. Choi, J. P. Sethna, M. D. Uchic, C. F. Woodward, and S. Zapperi, Quasi-periodic events in crystal plasticity and the self-organized avalanche oscillator, Nature (London) **490**, 517 (2012).
[30] E. A. Jagla, F. P. Landes, and A. Rosso, Viscoelastic Effects in Avalanche Dynamics: A Key to Earthquake Statistics, Phys. Rev. Lett. **112**, 174301 (2014).
[31] L. Laurson, X. Illa, and M. J. Alava, The effect of thresholding on temporal avalanche statistics, J. Stat. Mech. (2009) P01019.
[32] F. Font-Clos, G. Pruessner, N. R. Moloney, and A. DeLuca, The perils of thresholding, New J. Phys. **17**, 043066 (2015).

[33] M. Grob, J. Schmittbuhl, R. Toussaint, L. Rivera, S. Santucci, and K. J. Måløy, Quake catalogs from an optical monitoring of an interfacial crack propagation, Pure Appl. Geophys. **166**, 777 (2009).
[34] K. T. Tallakstad, L. Angheluta, S. Santucci, R. Toussaint, and K. J. Måløy (to be published).
[35] See Supplemental Material at http://link.aps.org/supplemental/10.1103/PhysRevLett.117.230601, which includes Refs. [36–40], for additional details of the simulations and experiments, and an analysis of a mean-field model.
[36] G. Durin and S. Zapperi, Universality and size effects in the Barkhausen noise, J. Appl. Phys. **87**, 7031 (2000).
[37] O. Duemmer and W. Krauth, Depinning exponents of the driven long-range elastic string, J. Stat. Mech. (2007) P01019.
[38] K. T. Tallakstad, R. Toussaint, S. Santucci, J. Schmittbuhl, and K. J. Måløy, Local dynamics of a randomly pinned crack front during creep and forced propagation: An experimental study, Phys. Rev. E **83**, 046108 (2011).
[39] A. Rosso, P. Le Doussal, and K. J. Wiese, Avalanche-size distribution at the depinning transition: A numerical test of the theory, Phys. Rev. B **80**, 144204 (2009).
[40] P. Le Doussal and K. J. Wiese, Driven particle in a random landscape: Disorder correlator, avalanche distribution, and extreme value statistics of records, Phys. Rev. E **79** 051105 (2009).
[41] D. Bonamy, S. Santucci, and L. Ponson, Crackling Dynamics in Material Failure as the Signature of a Self-Organized Dynamic Phase Transition, Phys. Rev. Lett. **101**, 045501 (2008).
[42] A. Tanguy, M. Gounelle, and S. Roux, From individual to collective pinning: Effect of long-range interactions, Phys. Rev. E **58**, 1577 (1998).
[43] D. Ertas and M. Kardar, Critical dynamics of contact line depinning, Phys. Rev. E **49**, R2532 (1994).
[44] J. F. Joanny and P. G. De Gennes, A model for contact angle hysteresis, J. Chem. Phys. **81**, 552 (1984).
[45] P. Moretti, M. C. Miguel, M. Zaiser, and S. Zapperi, Depinning transition of dislocation assemblies: Pileups and low-angle grain boundaries, Phys. Rev. B **69**, 214103 (2004).
[46] S. Papanikolaou, F. Bohn, R. L. Sommer, G. Durin, S. Zapperi, and J. P. Sethna, Universality beyond power laws and the average avalanche shape, Nat. Phys. **7**, 316 (2011).
[47] D. Sornette and M. J. Werner, Apparent clustering and apparent background earthquakes biased by undetected seismicity, J. Geophys. Res. **110**, B09303 (2005).